Journal of Non-Crystalline Solids 366 (2013) 35–41

Contents lists available at SciVerse ScienceDirect

Journal of Non-Crystalline Solids

journal homepage: www.elsevier.com/ locate/ jnoncrysol

Spectroscopic properties of Nd^{3+}-doped transparent glass ceramic containing $Sr_5(PO_4)_3F$ nanocrystals

S.N. Zhang [a,b], J.H. Huang [a], Y.J. Chen [a], X.H. Gong [a], Y.F. Lin [a], Z.D. Luo [a], Y.D. Huang [a,*]

[a] Key Laboratory of Optoelectronic Materials Chemistry and Physics, Fujian Institute of Research on the Structure of Matter, Chinese Academy of Sciences, Fuzhou, Fujian, 350002, China
[b] Graduate University of Chinese Academy of Sciences, Beijing 100039, China

ARTICLE INFO

Article history:
Received 23 November 2012
Received in revised form 24 January 2013

Keywords:
Oxyfluoride;
Thermal treatment;
$Sr_5(PO_4)_3F$ nanocrystals;
Laser material

ABSTRACT

A Nd^{3+}-doped transparent oxyfluoride glass ceramic containing $Sr_5(PO_4)_3F$ nanocrystals was prepared by melt quenching technique and subsequent thermal treatment. The phase and morphology of $Sr_5(PO_4)_3F$ nanocrystals were investigated by X-ray diffraction and transmission electron microscopy, respectively. The volume fraction of $Sr_5(PO_4)_3F$ nanocrystals in the glass ceramic is about 12% and the fraction of Nd^{3+} ions incorporated in the $Sr_5(PO_4)_3F$ nanocrystals is about 15%. The peak absorption cross-section increases to 145% at 806 nm and the full width at half maximum for the band around 806 nm decreases from 12.5 to 11 nm after the crystallization process. The 1059 nm peak stimulated emission cross-section increases from 2.27×10^{-20} to 3.07×10^{-20} cm^2 and the effective width for this band decreases from 35 to 30 nm after the crystallization process. The improvement of spectroscopic properties indicates that the glass ceramic is potentially applicable as a 1.06 μm laser material.

1. Introduction

Nd^{3+}-doped transparent glass ceramics have attracted much attention owing to their potential application in solid state laser [1,2]. The glass ceramics containing CaF_2, LaF_3, PbF_2, and YF_3 nanocrystals were widely investigated [3–6]. Such nanocomposites are obtained from precursor glasses by thermal treatment close to the crystallization temperature [7,8]. These materials may combine the luminescence characteristics of rare earth ions in crystalline environment with the easy fabrication, high mechanical, chemical and thermal stabilities of the glass [9,10]. The key factors for this combination are the incorporation of the rare earth ions in the precipitated nanocrystals and the maintenance of the transparency [11,12].

Laser with low threshold and high slope efficiency has been realized in fluorapatite crystals like Nd^{3+}:$A_5(PO_4)_3F$ (A = Ca, Sr) [13–16]. However, the poor thermomechanical properties and inadequate crystal quality of these fluorapatite crystals [17] make it hard to be applied as high power laser gain medium. Recently, a Nd^{3+}-doped transparent oxyfluoride glass ceramic containing $Ca_5(PO_4)_3F$ (FAP) nanocrystals has been prepared in our lab [18]. Some obvious improvements of spectroscopic properties of the glass ceramic were demonstrated after the crystallization process. To the author's knowledge, glass ceramics containing $Sr_5(PO_4)_3F$ (SFAP) nanocrystals have not been reported in the literature. Furthermore, the spectroscopic properties and laser performance of Nd^{3+}:SFAP crystal are better than that of Nd^{3+}:FAP crystal [16]. In this work, a Nd^{3+}-doped transparent oxyfluoride glass ceramic containing SFAP nanocrystals was prepared and the spectroscopic properties of Nd^{3+} ions in the glass ceramics were studied and compared with those in the glass ceramic containing FAP nanocrystals.

2. Experimental

The $29.4SiO_2$–$18.0Al_2O_3$–$12.0P_2O_3$–$20.0SrCO_3$–$18.0SrF_2$–$0.3La_2O_3$–$0.5Li_2CO_3$–$0.3B_2O_3$–$0.5ZrO_2$:$1.0Nd_2O_3$ (mol%) precursor glass (denoted as Nd^{3+}:PG) was prepared by melting a mixture of the reagents in an alumina crucible at 1480 °C for 2 h under air atmosphere. The reagents purity is shown in Table 1. The melt was quenched in a 280 °C preheated copper mold and then cooled to room temperature naturally. The transparent glass ceramic (denoted as Nd^{3+}:GC) was obtained through crystallization after heating Nd^{3+}:PG at 820 °C for 2 h. The sample densities were measured using the buoyancy method based on the Archimedes principle with the distilled water as the immersion liquid. The Nd^{3+} concentrations N can be evaluated by $N = 2dN_A\rho/M$, where d is the weight percent of Nd_2O_3, N_A is the Avogadro's constant, ρ is the sample density and M is the molar mass of Nd_2O_3. The Nd^{3+} concentrations in Nd^{3+}:PG and Nd^{3+}:GC were estimated to be about 3.69×10^{20} and 3.81×10^{20} ions/cm^3, respectively. Two samples with thicknesses of 1.97 and 1.98 mm were cut from Nd^{3+}:PG and Nd^{3+}:GC, respectively. All the surfaces of these samples were polished for optical experiments.

Differential scanning calorimetry (DSC) experiments were carried out with a DSC equipment (STA449C, Netzsch) at a heating rate of 10 °C/min. To identify the crystallization phase, X-ray diffraction (XRD) analysis was carried out with a powder diffractometer (DMAX2500, Rigaku) using a Cu rotating anode source. Sizes and morphologies of

* Corresponding author. Fax: +86 591 83715544.
E-mail address: huyd@fjirsm.ac.cn (Y.D. Huang).

0022-3093/$ – see front matter © 2013 Elsevier B.V. All rights reserved.
http://dx.doi.org/10.1016/j.jnoncrysol.2013.01.048

Table 1
The purity of the reagents.

Reagent	Purity (%)	Reagent	Purity (%)
SiO_2	99.99	La_2O_3	99.99
Al_2O_3	99.99	Li_2CO_3	97
P_2O_3	99.9	B_2O_3	98
$SrCO_3$	99	ZrO_2	99.99
SrF_2	99	Nd_2O_3	99.99

the Nd^{3+}:GC sample were measured by a transmission electron microscope (TEM) (JEM-2010, JEOL). TEM specimen was prepared by dispersing the fine powder grinded from the bulk sample in ethanol, followed by ultrasonic dispersion, and then depositing onto the carbon of the copper grid. Absorption and transmission spectra were performed in a spectrophotometer (Lambda35, Perkin-Elmer) at room temperature. Emission spectra were performed using a spectrometer (FL920, Edinburgh) by pumping samples with a Ti:sapphire laser (Model 3900 s, Spectra-Physics) at room temperature and at 5 K. Transmission spectra at 3 K were recorded by a spectrophotometer (1000 M, SPEX). Room temperature fluorescence decay curves of the $^4F_{3/2}$ level from Nd^{3+} ions were recorded with a near infrared photomultiplier tube (R5509, Hamamatsu) by exciting samples at 806 nm with a microsecond flash lamp (μF900, Edinburgh).

3. Results and discussion

Fig. 1 shows the DSC curve of Nd^{3+}:PG sample, where T_g (727 °C), T_{c1} (820 °C) and T_{c2} (905 °C) stand for the glass transition temperature and the crystallization temperatures for SFAP and mullite [19], respectively. For comparison, the DSC curve of an undoped PG sample is also shown in Fig. 1. It can be seen that the undoped PG has similar glass transition temperature (730 °C) and crystallization temperatures (816 °C and 900 °C). Although the crystallization peaks did not move like those between the undoped and Nd_2O_3 doped FAP glasses [18], the undoped PG sample gives relatively large and intense crystalline exothermic peaks. It indicates that the dopant Nd_2O_3 may difficult the crystallization of SFAP and mullite phases in the Nd^{3+}:PG samples. Furthermore, when compared with the crystallization temperature for the FAP glass [18], the SFAP in PG has a higher crystallization temperature, which is closer to the crystallization temperature of mullite. A long crystallization time, as much as 24 h for the Nd^{3+}:FAP glass ceramic [18], would make the Nd^{3+}:PG loss its transparency due to the crystallization of mullite. Therefore, the Nd^{3+}:PG was heated at 820 °C for only 2 h for the crystallization of SFAP. Fig. 2 displays the XRD pattern of the Nd^{3+}:GC. All diffraction peaks matched well with the standard data of hexagonal phase SFAP (JCPDS 17-0609). The TEM image of the Nd^{3+}:GC shown in Fig. 3 exhibits that the SFAP nanocrystals have a 20–50 nm size range and they are embedded in the glass matrix.

The photographs of the Nd^{3+}:PG and Nd^{3+}:GC samples for spectral experiments are shown in the insets of Fig. 4, which display that the Nd^{3+}:PG and Nd^{3+}:GC are transparent in the visible range. As shown in Fig. 4 the transmittances of the Nd^{3+}:PG and Nd^{3+}:GC reach 84.4% and 69.5%, respectively, at 633 nm without considering the absorption of Nd^{3+} ions. The transmittance of Nd^{3+}:GC at wavelength λ, where there is not any absorption of Nd^{3+} ions, can be evaluated by [20,21]

$$T = \exp\left\{-\frac{32\pi^4\varphi_c x r^3 n_{pg}^4}{\lambda^4}\left[\frac{\left(n_s/n_{pg}\right)^2-1}{\left(n_s/n_{pg}\right)^2+2}\right]^2\right\} \quad (1)$$

where ϕ_c is volume fraction of SFAP nanocrystals, r is the average size of SFAP nanocrystals and 35 ± 5 nm was adopted based on the TEM image, x is the optical path length and was equivalent to the sample thickness, n_s is the average refractive index of SFAP crystal and was calculated following $n_s=(2n_\sigma+n_\pi)/3$, where n_σ and n_π are the refractive indices for σ and π polarizations, respectively [22], and n_{pg} is the refractive index of PG. Since the PG composition is similar to that of the FAP glass, and the difference between the refractive indices of FAP crystal and SFAP crystal is only around 0.002 [18,22], the refractive indices of Nd^{3+}:FAP glass and Nd^{3+}:FAP glass ceramic in Ref. [18] were adopted for Nd^{3+}:PG and Nd^{3+}:GC, respectively. From the 69.5% transmittance of Nd^{3+}:GC at 633 nm, the volume fraction of SFAP nanocrystals ϕ_c could be estimated to be about (12 ± 3)%. Compared with that for the Nd^{3+}:FAP glass ceramic [18], the lower volume fraction of SFAP nanocrystals for Nd^{3+}:GC is probably caused by the shorter crystallization time. This result also reveals that the lower transmittance of Nd^{3+}:GC than that of the Nd^{3+}:FAP glass ceramic [18] is mainly caused by the larger size of SFAP nanocrystals [23].

The room temperature absorption spectra of Nd^{3+} ions for Nd^{3+}:PG and Nd^{3+}:GC are shown in Fig. 5. The absorption bands are corresponding to the transitions from the ground multiplet $^4I_{9/2}$ and the final multiplets marked in the figure. The peak absorption cross-section at 806 nm of Nd^{3+}:GC increases up to 145% of that at 803 nm of Nd^{3+}:PG. The larger absorption cross-section is beneficial to a laser gain medium pumped by diode laser with narrow spectral width [5,6,18]. The full width at half maximum (FWHM) of the absorption band around 806 nm for Nd^{3+}:GC has been determined to be about 11 nm by adjusting Gaussian curves, which is narrower

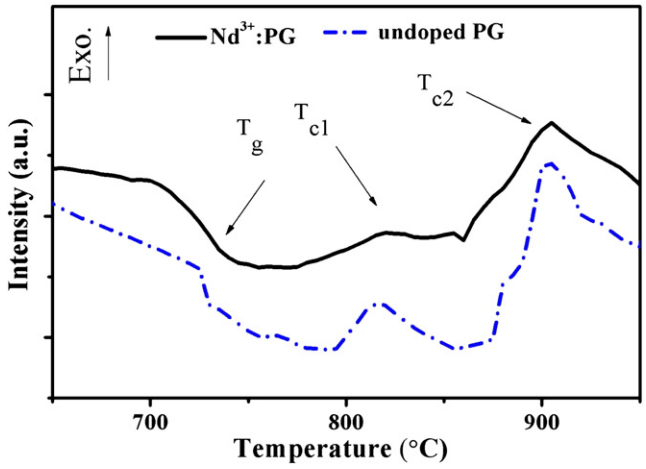

Fig. 1. DSC curves of Nd^{3+}:PG and undoped PG.

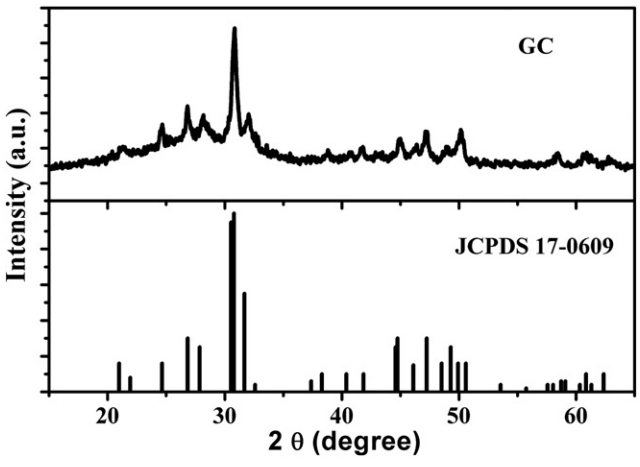

Fig. 2. XRD pattern of Nd^{3+}:GC. The bars represent the diffraction pattern of the standard hexagonal phase SFAP.